Carcinogenesis vol.31 no.5 pp.902–910, 2010
doi:10.1093/carcin/bgq039
Advance Access publication February 16, 2010

Pro-oxidative activities and dose–response relationship of (−)-epigallocatechin-3-gallate in the inhibition of lung cancer cell growth: a comparative study *in vivo* and *in vitro*

Guang-Xun Li, Yu-Kuo Chen, Zhe Hou[1], Hang Xiao[2], Huanyu Jin, Gary Lu, Mao-Jung Lee, Ba Liu, Fei Guan, Zhihong Yang, Albert Yu and Chung S.Yang*

Susan Lehman Cullman Laboratory for Cancer Research, Department of Chemical Biology and Center for Cancer Prevention Research, Ernest Mario School of Pharmacy, Rutgers, The State University of New Jersey, Piscataway, NJ 08854, USA

[1]Present address: Department of Medicine, Weill Medical College of Cornell University, New York, NY 10021, USA

[2]Present address: Department of Food Science, University of Massachusetts Amherst, 100 Holdsworth Way, Amherst, MA 01003, USA

*To whom correspondence should be addressed. Department of Chemical Biology, Ernest Mario School of Pharmacy, Rutgers, State University of New Jersey, 164 Frelinghuysen Road, Piscataway, NJ 08854-8020, USA.
Tel: +1 732 445 5360; FAX: +1 732 445 0687;
Email: csyang@rci.rutgers.edu

(−)-Epigallocatechin-3-gallate (EGCG), the major polyphenol in green tea, has been shown to inhibit tumorigenesis and cancer cell growth in animal models. Nevertheless, the dose–response relationship of the inhibitory activity *in vivo* has not been systematically characterized. The present studies were conducted to address these issues, as well as the involvement of reactive oxygen species (ROS), in the inhibitory action of EGCG *in vivo* and *in vitro*. We characterized the inhibitory actions of EGCG against human lung cancer H1299 cells in culture and in xenograft tumors. The growth of tumors was dose dependently inhibited by EGCG at doses of 0.1, 0.3 and 0.5% in the diet. Tumor cell apoptosis and oxidative DNA damage, assessed by the formation of 8-hydroxy-2′-deoxyguanosine (8-OHdG) and phosphorylated histone 2A variant X (γ-H2AX), were dose dependently increased by EGCG treatment. However, the levels of 8-OHdG and γ-H2AX were not changed by the EGCG treatment in host organs. In culture, the growth of viable H1299 cells was dose dependently reduced by EGCG; the estimated concentration that causes 50% inhibition (IC_{50}) (20 μM) was much higher than the IC_{50} (0.15 μM) observed *in vivo*. The action of EGCG was mostly abolished by the presence of superoxide dismutase (SOD) and catalase, which decompose the ROS formed in the culture medium. Treatment with EGCG also caused the generation of intracellular ROS and mitochondrial ROS. Although EGCG is generally considered to be an antioxidant, the present study demonstrates the pro-oxidative activities of EGCG *in vivo* and *in vitro* in the described experimental system.

Introduction

Tea (*Camellia sinensis)* is a popular beverage worldwide. Green tea contains characteristic polyphenol constituents, generally known as catechins, which include (−)-epigallocatechin-3-gallate (EGCG), (−)-epicatechin-3-gallate, (−)-epigallocatechin and (−)-epicatechin. Of these catechins, EGCG is the most abundant and biologically active compound in green tea. Although the cancer preventive activity of tea polyphenols has been demonstrated in many experimental systems (reviewed in refs 1–4), the dose–response relationship *in vivo* has not been clearly established. In the literature, a wide range of concentrations of EGCG or green tea polyphenols had been reported to inhibit tumorigenesis in animal models or to inhibit the growth of xenograft tumors. Some studies have showed inhibitory activity at concentrations as low as 0.04% EGCG in drinking fluid (5,6), whereas some other studies have reported much higher concentrations, for example 1% tea solids (containing 0.3% green tea polyphenols) or higher, to demonstrate an inhibitory effect *in vivo* (7–9). Some studies have relied on intraperitoneal (i.p.) injections of EGCG to demonstrate inhibitory effects on tumor growth (10,11). In studies with cell lines, most experiments have used EGCG concentrations in the range of 5–100 μM. However, in animal studies, when the blood levels of EGCG have been measured, the concentrations of EGCG are usually <0.5 μM (12). The lack of understanding of the dose–response relationship in the inhibition of tumorigenesis or tumor growth *in vivo*, as well as the relationship between effective inhibitory concentrations of EGCG *in vivo* and *in vitro*, made it difficult to evaluate the relevance of the many studies conducted *in vitro* (4).

In previous studies, we have demonstrated that EGCG is readily auto-oxidized in cell culture medium to produce superoxide, H_2O_2, and perhaps other reactive oxygen species (ROS) (13,14). These ROS can induce cellular damage and cell death, and these actions can be prevented or attenuated by the addition of superoxide dismutase (SOD) and catalase (13–15). As we reviewed previously, animal tissue is generally endowed with antioxidant enzymes and is usually under lower oxygen partial pressure than the cell culture medium (16). It is not clear whether this type of pro-oxidative action of EGCG occurs in animal tissues. Therefore, a careful comparative *in vivo* and *in vitro* study is needed.

ROS are known to produce oxidative stress and cause damage to DNA and other cellular molecules (17). The oxidative DNA product, 8-hydroxy-2′-deoxyguanosine (8-OHdG), is a commonly used marker for oxidative stress in tissues (18). ROS can also cause DNA double-strand breaks, which activate ataxia-telangiectasia-mutated as well as ataxia-telangiectasia-mutated- and Rad3-related kinases (19,20). Activated ataxia-telangiectasia-mutated can phosphorylate H2AX, a variant of histone H2A, at Ser139. The phosphorylated histone 2A variant X (γ-H2AX) can form nuclear foci surrounding the damage sites and help to recruit DNA repair machinery (21–23). In response to double-strand break, γ-H2AX is formed rapidly. Therefore, γ-H2AX has been used as a sensitive marker for the presence of double-strand break in cells and tissues (24,25).

In this study, we characterized the dose–response relationship of EGCG in the inhibitory action against human lung cancer H1299 cells, as well as the involvement of oxidative stress, in a cell culture system and in a xenograft model. The results, especially the effective inhibitory concentrations of EGCG, *in vitro* and *in vivo* were compared. The EGCG-induced oxidative stress was observed in cancer cells in both systems, but the effective concentration *in vitro* was found to be at two orders of magnitude higher that those observed *in vivo*.

Materials and methods

Animals and xenograft model in vivo experiment

Male NCr nu/nu mice (Taconic Farms, Germantown, NY) were maintained on the AIN93M diet (Research Diets, New Brunswick, NJ). At 6 weeks of age, five groups of mice ($n = 10$) were injected subcutaneously with H1299 (1×10^6 cells) on both flank sides. Three groups of mice were maintained on the AIN93M diet supplemented with 0.1, 0.3 and 0.5% EGCG, respectively. The fifth group received EGCG through daily i.p. injections at 30 mg/kg body wt. EGCG (94% pure) was a gift from Dr Y.Hara (Mitsui Norin Co., Fujieda city, Shizuoka, Japan). Tumor volume, body weight and food consumption were monitored twice weekly. Tumor size was measured by a caliper and calculated based on tumor volume (length × width^2 × 0.5). On day 45, the mice were

Abbreviations: IC_{50}, concentration that causes 50% inhibition; MTT, 3-(4,5-Dimethylthiazole-2-yl)-2,5-diphenyltetrazolium bromide; EGCG, (−)-epigallocatechin-3-gallate; i.p., intraperitoneal; 8-OHdG, 8-hydroxy-2′-deoxyguanosine; NAC, *N*-acetyl-cysteine; γ-H2AX, phosphorylated histone 2A variant X; ROS, reactive oxygen species; SOD, superoxide dismutase.

killed by CO_2 asphyxiation between 9 and 11 a.m. The tumors were dissected. One half of tumor was fixed in 10% buffered formalin for immunohistochemistry and the second half was snap frozen for biochemical analysis. The liver, lung, kidney and serum samples were collected.

Plasma and tissue levels of EGCG

The samples were analyzed using a procedure described previously (26). In brief, the tissue samples, ~0.1 g, were homogenized with 0.05 ml of 1% ascorbic acid and 0.45 ml of methanol:ethyl acetate (2:1) and centrifuged. The supernatant (500 µl) or plasma (200 µl) was extracted with 1 ml hexane twice. After the second extraction, the sample was mixed with 10 µl of 0.2% ascorbic acid and dried. The dried sample was reconstituted in 100 µl 10% aqueous acetonitrile solution, and 50 µl of the sample were injected onto the high-performance liquid chromatography system. The results are expressed on the basis of plasma volume or wet weight of tissues.

Cell culture

Human non-small-cell lung cancer-derived cell line H1299, human large-cell lung cancer-derived cell line H460, human lung carcinoma-derived cell line A549 and human colorectal adenocarcinoma-derived cell line HT29 were purchased from American Type Culture Collection (Manassas, VA). CL13 mouse lung adenocarcinoma cells were generously provided by Dr Steven A.Belinsky (Lovelace Respiratory Research Institute, Albuquerque, NM). H1299, H460 and CL13 cells were maintained in RPMI-1640 medium with 10% fetal bovine serum. A549 cells were maintained in F-12K medium with 10% fetal bovine serum and HT29 cells were maintained in McCoy's 5A medium with 10% fetal bovine serum. All cells were maintained in 5% CO_2 humidified atmosphere at 37°C. Cell cultures used for experiments were at 60–70% confluence, which was usually achieved 24 or 48 h after plating. EGCG was dissolved in double-deionized filter-sterilized water. For treatment, the cells were incubated with 5–50 µM of EGCG in a fresh serum-free medium in the presence or absence of SOD (5 U/ml) and catalase (30 U/ml) for different periods of time at 37°C. 3-(4,5-Dimethylthiazole-2-yl)-2,5-diphenyltetrazolium bromide (MTT) (Sigma, St Louis, MO) assay was performed by following the manufacturer's instruction.

Immunohistochemistry and immunocytochemistry

Deparaffinized sections were unmasked in antigen-unmasking solution (DAKO, Copenhagen, Denmark) in a microwave oven for antigen retrieval. Endogenous peroxidase was quenched using 3% H_2O_2 and then blocked for 1 h at room temperature and incubated with primary antibody overnight at 4°C. Biotin-conjugated secondary antibody (1:200) and avidin–biotin peroxidase complex (1:100) were then applied. Antibodies against γ-H2AX (1:400, Cell signaling, Danvers, MA), 8-OHdG (1:100, JaICA, Shizuoka, Japan) and cleaved caspase-3 (1:300, Cell signaling Technology) were used for the analysis. For each slide, 10 representative ×200 power photomicrographs were taken and positive-stained cancer cells and total number of cells were analyzed with the ImagePro+ image processing program. For immunocytochemistry, the cell slides were immersed in 0.2% Triton X-100 for 10 min and then blocked for 30 min. The cell slides were then incubated with primary γ-H2AX antibody (1:500) overnight at 4°C, washed and then incubated with secondary IgG–fluorescein isothiocyanate (1:5000, Sigma) for 1 h at room temperature. Parallel samples were incubated with anti-8-OHdG antibody (1:250) overnight at 4°C, washed and incubated with secondary antibody for 45 min at room temperature. The slides were then washed with phosphate-buffered saline and incubated with avidin–biotin peroxidase complex reagent for 30 min and stained with 3,3′-diaminobenzidine substrate reagent for 1 min in room temperature. Each experiment was performed with an IgG control.

Annexin V-fluorescein isothiocyanate and propidium iodide Costaining

Following the treatment, H1299 cells were harvested by trypsinization and washed cell pellets were resuspended in binding buffer (10 mM *N*-2-hydroxyethylpiperazine-*N*′-2-ethanesulfonic acid/NaOH, 140 mM NaCl and 2.5 mM $CaCl_2$, pH 7.4) with density adjusted to 2–5 × 10^5 cells/ml. A portion of the cell suspension (190 µl) was mixed gently with 10 µl annexin V-fluorescein isothiocyanate (Molecular Probes, Invitrogen, South San Francisco, CA) and incubated at room temperature for 15 min. The cells were centrifuged and resuspended in 190 µl binding buffer containing 1 µg/ml propidium iodide. Within 15 min of the last staining, the cells were analyzed by flow cytometry (Cytomics® FC500; Beckman Coulter, Miami, FL) at the Analytical Cytometry Core Facility and the data was processed using CXP acquisition and analysis software.

Western blots for γ-H2AX in cell lines and animal tissues

EGCG-treated cells were lysed in RIPA lysis buffer (Boston Bio-products, Worcester, MA) with phosphatase and protease inhibitors (Sigma). The tumor, liver, lung and kidney tissues were ground in glass douncers and lysed in T-Per tissue extraction buffer (Pierce, Rockford, IL) with protease and phosphatase inhibitors. The protein samples were loaded onto 12% sodium dodecyl sulfate–polyacrylamide gel electrophoresis gels. The proteins on the membranes were subsequently blocked with Commercial Li-Cor Blocking Buffer (Li-Cor Biotechnologies, Lincoln, NE) for 1 h at room temperature. The membranes were blotted with primary antibody γ-H2AX and β-actin (Sigma) antibody overnight at 4°C. The membranes were then incubated with fluorescence-conjugated secondary antibodies (Molecular Probes, Eugene, OR) for 1 h at room temperature. The fluorescent bands were detected by Odyssey® Infrared Imaging System (Li-Cor Biotechnologies).

Measurement of intracellular ROS, mitochondrial ROS and mitochondrial membrane potential changes

For the measurement of intracellular and mitochondrial ROS, the cells were incubated with 25 or 50 µM of EGCG in the presence or absence of SOD (5 U/ml) and catalase (30 U/ml) or *N*-acetyl-cysteine (NAC) (2 mM) with serum-free RPMI-1640 medium for 24 h at 37°C. H_2O_2 (100 µM) was used as positive control. For intracellular ROS, the cells were treated with 5 µM 2′,7′-dichlorodihydrofluorescein diacetate (D399; Molecular Probes, Carlsbad, CA) in cell medium for 15 min at 37°C. Live cell mitochondrial ROS was determined by MitoSOX red dye (M36008; Invitrogen) for 10 min. The cells were harvested by trypsinization, and washed cell pellets were resuspended in phosphate-buffered saline for analysis by flow cytometry. To determine the percentage of cells with collapsed mitochondrial membrane potential, $DiOC_6$ dye (Molecular Probes, Carlsbad, CA) was used. Cells were treated with EGCG as above, harvested by trypsinization and washed once with phosphate-buffered saline, and $DiOC_6$ dye was added to a final concentration of 50 nM. After 15 min of incubation at 37°C, the relative fluorescence intensity was measured using flow cytometry.

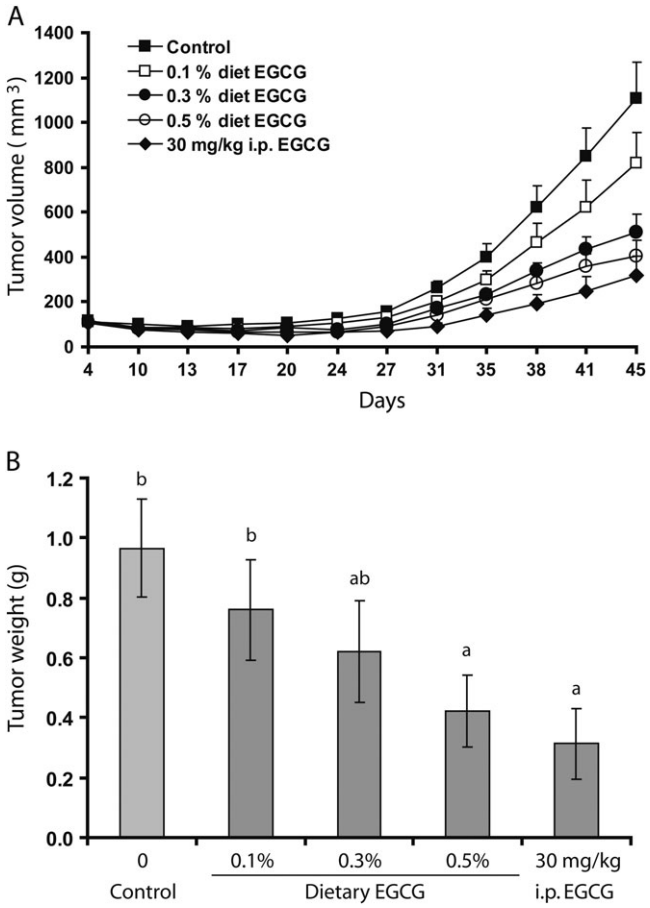

Fig. 1. Inhibitory effects of EGCG treatments on the growth of H1299 lung cancer cell xenografts. (**A**) Mean tumor volume as a function of time. (**B**) Final tumor weight. The values shown are mean ± SE of 10 mice (20 tumors) per group. Different superscripts (a and b) indicate statistical difference among groups (by one-way analysis of variance; $P < 0.05$).

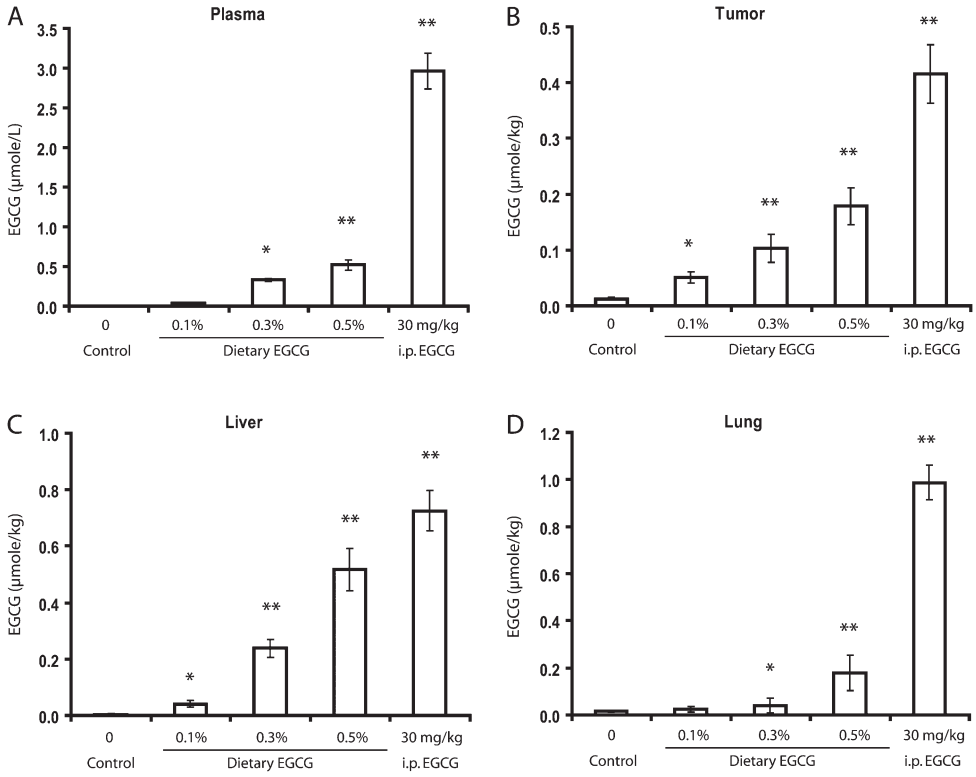

Fig. 2. EGCG levels in the plasma (**A**), tumor (**B**), liver (**C**) and lung (**D**). The values are shown as mean ± SE of 10 mice. Statistical significance from control group by two-tailed *t*-test: $^{*}P < 0.05$ and $^{**}P < 0.01$.

Data analysis

All data was presented as mean ± SD or mean ± SE Student's *t*-test was used to test the difference between two groups. Statistical significance was indicated by $P < 0.05$ in the two-tailed comparison. Analyses of variance model was used for the comparison of the differences among more than two groups. The linear regression analysis was performed using SigmaPlot 8.0.

Results

Dose–response inhibition of H1299 xenograft tumor growth by EGCG

In this study, five groups of mice were used. No difference in feed intake and body weight gain was observed among the different EGCG treatment groups. As shown in Figure 1A, EGCG treatment inhibited tumor growth during the 45 day experimental period. At the end of the experiment, the tumor weights were significantly lower in the 0.5% dietary EGCG group (by 56.7%, $P < 0.05$) as compared with the control group (Figure 1B). A linear regression analysis showed that the tumor weight was dose dependently decreased by the treatment with dietary EGCG ($y = 0.920 - 1.014x$, $R^2 = 0.965$; where y is the tumor weight in grams and x is the dietary EGCG content in percentages). As a comparison, the fifth group was treated by daily i.p. injection of 30 mg/kg body wt, and a significant inhibition (by 68.0%, $P < 0.05$) was also observed.

EGCG levels in the blood, tumor and tissues

With increased dietary EGCG levels from 0.1 to 0.5%, the EGCG levels in the plasma, xenograft tumor, liver and lungs dose dependently increased; i.p. administration of EGCG at 30 mg/kg raised the plasma and tissues EGCG to ever higher levels (Figure 2). The observed plasma levels for the 0.1, 0.3 and 0.5% dietary EGCG groups and the 30 mg/kg i.p. injection group were 0.03, 0.33, 0.52 and 2.96 2μmol/l, respectively (Figure 2A). The EGCG levels in the xenograft tumors were 0.05, 0.10, 0.18 and 0.42 μmol/kg, respectively (Figure 2B); in the liver were 0.04, 0.24, 0.52 and 0.73 μmol/kg, respectively (Figure 2C) and in the lung were 0.02, 0.04, 0.18 and 0.99 μmol/kg, respectively (Figure 2D). Since these are the results of treatment for 44 days, there values represent steady state levels of mouse tissue levels of EGCG at the time of sacrifice (between 9 and 11 a.m.). It is known that after dietary administration of EGCG, it takes 90–120 min for EGCG to reach peak levels in the blood and that EGCG clears from the blood with an elimination half-life of 3–4 h (12). The mice are nocturnal with eating time mostly at night (6 p.m. to 6 a.m.). Since the blood samples were collected at 9–11 a.m., our observed plasma values may be half of the peak levels (e.g. at 6 a.m.) and three or four times higher than the levels at 6 p.m. A linear regression analysis on the dietary EGCG-treated groups showed that the tumor weight was dose dependently decreased with the increase in tumor EGCG concentration ($y = 0.940 - 2.99x$, $R^2 = 0.973$; where y is the tumor weight in grams and x is the tumor EGCG concentration in micromole per kilogram). Based on this regression analysis, the concentration that causes 50% inhibition (IC_{50}) is calculated to be 0.15 μmol/kg. Assuming a value of 1 l for 1 kg tumor, 0.15 μmol/kg is equal to 0.15 μM. The i.p. injection took place 2 h before the mice were killed; therefore, the observed plasma EGCG values were close to the peak values. The plasma levels of EGCG in the i.p. injected EGCG group were 5-fold higher than the 0.5% dietary EGCG group. A large difference between the i.p. EGCG group and dietary EGCG groups was also observed in the lung EGCG levels, whereas the difference between the two groups was not as big in the liver and tumor EGCG levels.

Induction of oxidative stress, DNA damage-induced repair and apoptosis in xenograft tumors

The possible induction of oxidative stress, DNA damage-induced repair and apoptosis by EGCG was assessed by immunohistochemistry staining of 8-OHdG, γ-H2AX and cleaved caspase-3, respectively, in the xenograft tumors. A dose-dependent induction of all these parameters by EGCG treatment was observed (Figure 3). On the contrary, an induction of 8-OHdG formation was not observed in host mouse lung (by immunohistochemistry); the induction of

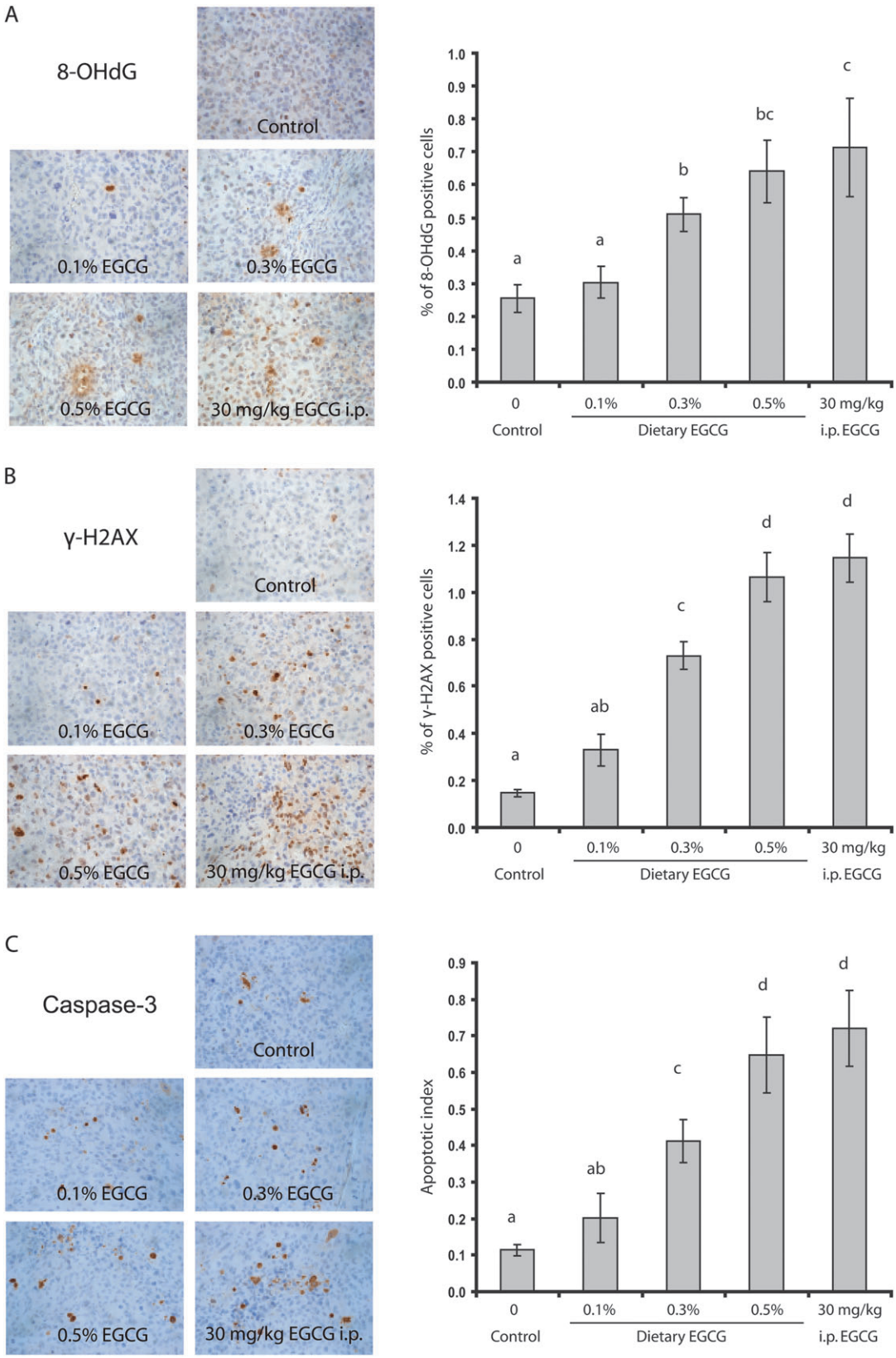

Fig. 3. Effects of EGCG treatments on oxidative stress, DNA damage repair and apoptosis in the xenograft tumors. Representative immunohistochemisty microphotographs and percentage for 8-OHdG-positive-stained cells (**A**) and γ-H2AX-positive-stained cells (**B**) and apoptotic index **(C)**. Values in the bar graphs represent mean ± SE ($n = 6$ mice). Different superscripts (a, b, c and d) indicate statistical difference among groups (by one-way analysis of variance; $P < 0.05$).

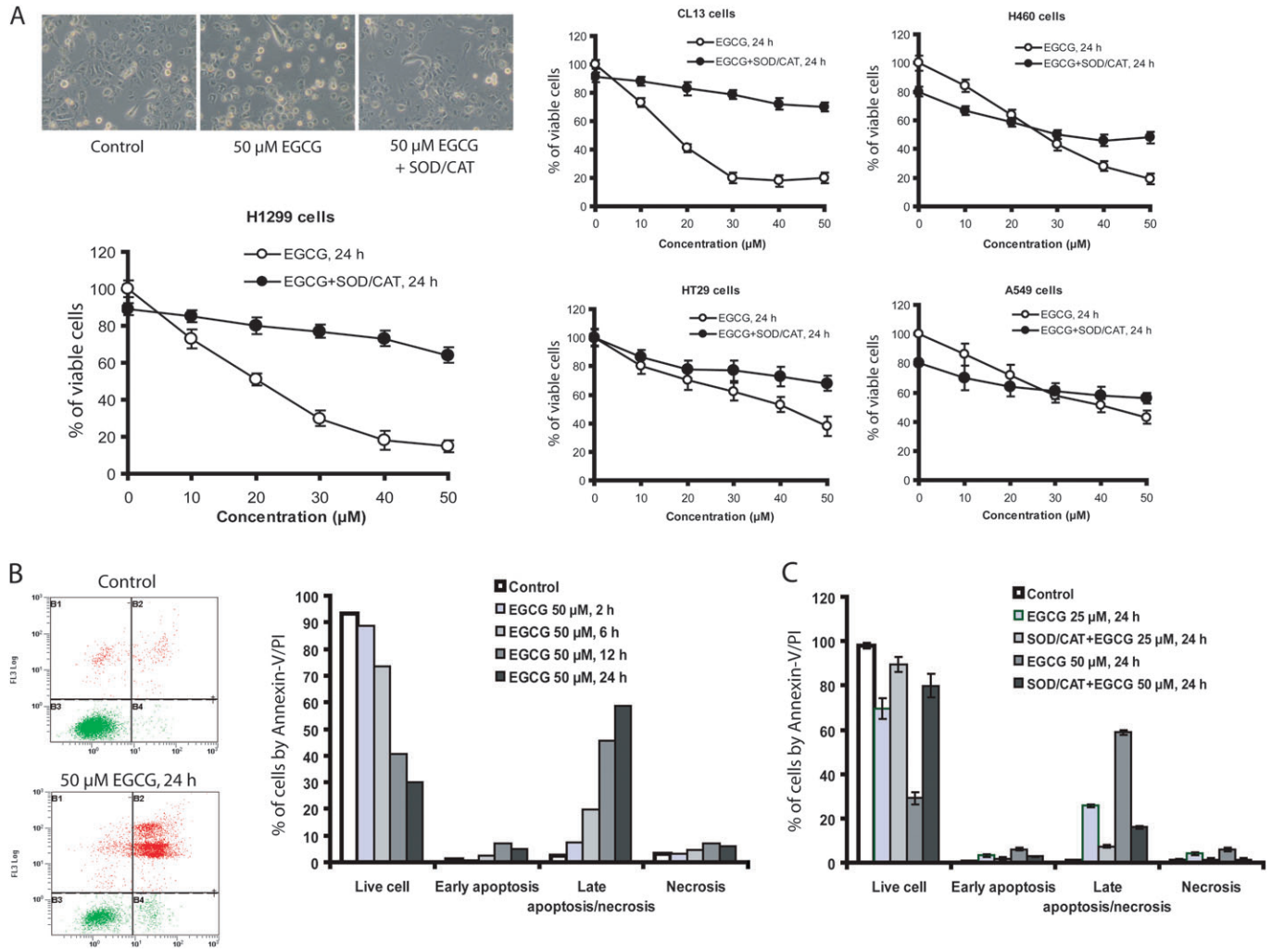

Fig. 4. Inhibition of cancer cells growth and induction of apoptosis by EGCG. (**A**) Morphological change of H1299 cells and percentage of viable cells for H1299, CL13, A549, H460 and HT29 ($n = 3$) after treatment with EGCG for 24 h in serum-free medium with (closed circles) or without (open circles) added SOD/catalase (CAT) (5 U/ml, 30 U/ml). (**B**) Annexin-V/propidium iodide (PI) costained cells after treatment with 50 μM EGCG for different time periods and **(C)** with 25 or 50 μM EGCG for 24 h in the presence or absence of SOD/CAT in serum-free medium. The values shown are mean ± SD.

γ-H2AX was also not observed in the liver or kidney (by western blots) (data not shown).

Effects of EGCG on cancer cell growth and apoptosis

In this comparative study, the inhibitory action of EGCG was also investigated in cell cultures by MTT assay. H1299 cells were treated with different concentrations of EGCG in serum-free medium for 24 h. As shown in Figure 4A, the numbers of viable H1299 cells were dose dependently decreased by EGCG, showing an estimated IC_{50} of 20 μM. The presence of SOD/catalase (5 U/ml, 30 U/ml) markedly attenuated the inhibitory actions of EGCG. Similar studies were also conducted with lung cancer cell lines, CL13 (mouse), H460 (human) and A549 (human), and colon cancer cell line HT29 (human). CL13 cells appeared to be slightly more susceptible, and H460 cells less susceptible, than H1299 cells to the inhibition by EGCG. The inhibitory activity was also markedly attenuated by the addition of SOD and catalase. On the other hand, the A549 and HT29 cells were less responsive to the inhibition by EGCG, and the effect of SOD/catalase was less pronounced, suggesting that EGCG-generated ROS plays a less important role in reducing the number of viable cells as compared with the system with H1299 cells.

Annexin-V/propidium iodide apoptosis data showed that when H1299 cells were incubated with 50 μM EGCG, cells at early or late stages of apoptosis and in necrosis were increased with time in the 24 h treatment period (Figure 4B). In H1299 cells treated with 25 or 50 μM of EGCG for 24 h, the presence of SOD/catalase (5 U/ml, 30 U/ml) significantly decreased the number of cells in the early apoptosis, late apoptosis and necrosis states ($P < 0.05$) (Figure 4C). The data suggest that the cell death is caused by ROS produced by EGCG auto-oxidation in the cell culture medium.

Generation of ROS by EGCG

The intracellular levels of ROS produced by the incubation of H1299 cells with 25 or 50 μM EGCG was investigated. Figure 5A shows representative fluorescence images of the cells after incubation with EGCG for 6 h. Figure 5B shows that EGCG induced a time-dependent production of intracellular ROS. In both sets of experiments, the number of ROS-positive cells was significantly decreased by the presence of SOD and catalase in the incubation. The presence of SOD/catalase markedly reduced the number of ROS-positive cells due to treatment with EGCG for 12 or 24 h (Figure 5B and C). Nevertheless, even in the presence of SOD/catalase, there were still substantial levels of ROS, especially in the cells that had been incubated with EGCG for 24 h. The presence of 2 mM NAC in the culture medium, however, was effective in reducing the number of ROS-positive cells to the control levels at both time points (Figure 5C). Because of the molecular sizes of SOD and catalase, these proteins are not expected to enter into the cells during incubation. SOD/catalase, therefore, can

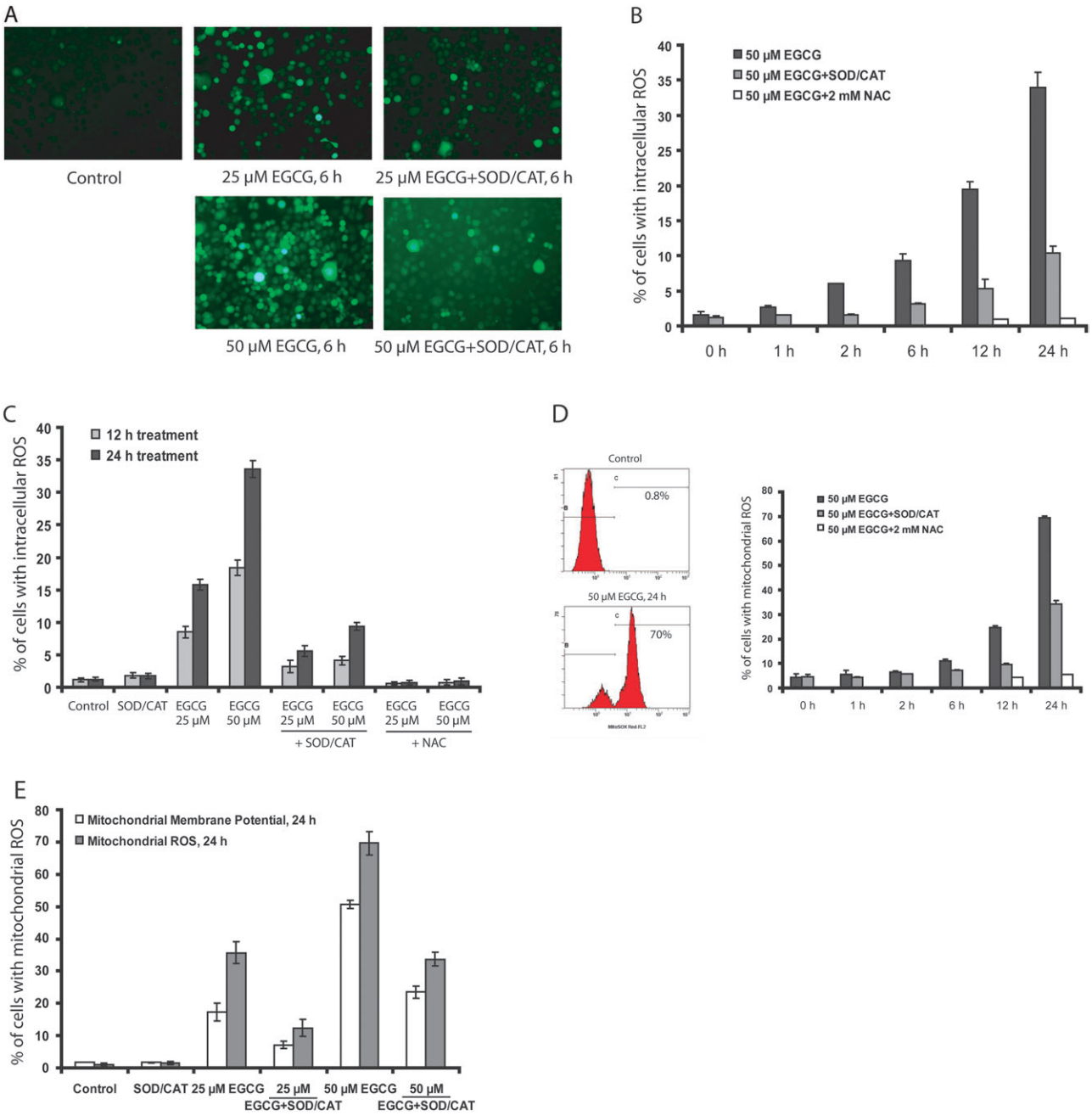

Fig. 5. Induction of intracellular ROS, mitochondrial ROS and mitochondrial membrane potential change by EGCG in H1299 cells. (**A**) Representative fluorescence images of intracellular ROS after induction for 6 h. (**B**) Time-dependent generation of intracellular ROS. (**C**) Intracellular ROS formation in the presence or absence of SOD/catalase (CAT) (5 U/ml, 30 U/ml) or NAC (2 mM) for 12 and 24 h. (**D**) Flow cytometry representative histogram and time-dependent generation of mitochondrial ROS with 25 or 50 μM of EGCG in the presence or absence of SOD/CAT. (**E**) Comparison of mitochondrial membrane potential change and mitochondrial ROS production with 25 or 50 μM of EGCG in the presence or absence of SOD/CAT for 24 h. The values shown are mean ± SD.

only quench the ROS generated in the culture medium outside of the cells, whereas NAC can quench ROS generated both inside and outside of the cells. Thus, the ROS generated in the presence of SOD/catalase, which can be quenched by NAC, may reflect the ROS generated intracellularly caused by the EGCG treatment.

Mitochondrial ROS and mitochondrial membrane potential changes caused by EGCG

Mitochondrial ROS levels and mitochondrial membrane potential changes were measured. A time-dependent formation of mitochondrial ROS was observed after incubation of H1299 cells with 50 μM EGCG, and mitochondrial ROS was decreased by the presence of SOD/catalase (by ∼50%) (Figure 5D). The presence of NAC effectively decreased mitochondrial ROS to the control level (Figure 5D). Treatment with EGCG also caused mitochondrial membrane potential changes, and these changes were attenuated by ∼50% by the presence of SOD/catalase (Figure 5E). These results suggest that the mitochondrial ROS and membrane potential change are caused by ROS generated extracellularly, as well as by ROS produced intracellularly.

Induction of 8-OHdG and γ-H2AX formation by EGCG in cultured cells

In order to examine the involvement of oxidative stress and DNA damage in EGCG-induced apoptosis in H1299 cells, we measured

8-OHdG and γ-H2AX levels after treatment with EGCG for 12 and 24 h. Treatment with 50 μM EGCG induced 8-OHdG and γ-H2AX formation, and the levels were reduced in the presence of SOD/catalase (Figure 6A). When cells were incubated with 5, 25 and 50 μM EGCG for 3–48 h, the formation of γ-H2AX was blocked by the presence of SOD/catalase. At 3 h, the formation of γ-H2AX was apparent only with 50 μM EGCG and at 12 h, induction of γ-H2AX by 25 μM EGCG was also observed. At both 3 and 12 h, the presence of SOD/catalase decreased the formation of γ-H2AX. At 24 h, EGCG appeared to dose dependently produce γ-H2AX, which was partially blocked by SOD/catalase. At 48 h, higher levels of γ-H2AX were produced with all three concentrations of EGCG, and SOD/catalase did not show any inhibition. It is probably that the γ-H2AX observed at 3 and 12 h were caused by ROS generated from EGCG auto-oxidation, whereas at the later time points, it was produced mainly intracellularly during apoptosis.

Discussion

The present study clearly demonstrates that EGCG dose dependently inhibited the growth of H1299 cells in cell culture and in xenograft tumors, and EGCG induced ROS formation in both the *in vitro* and *in vivo* systems. To our knowledge, this is the first demonstration that EGCG induces ROS formation and consequently causes DNA oxidative damage in tumor cells in animals.

As was reviewed previously, many mechanisms have been proposed for the inhibitory action of EGCG against cancer formation and growth (4). Chemically, there are two possible types of mechanisms. One is that EGCG binds to protein targets and then directly or indirectly blocks signaling pathways important for carcinogenesis or cancer cell growth. EGCG target proteins or high affinity binding proteins, such as laminin receptor (27), vimentin (28), insulin-like growth factor 1 receptor (29) and FYN (30), have been characterized. A second type of mechanism for the action of EGCG involves the

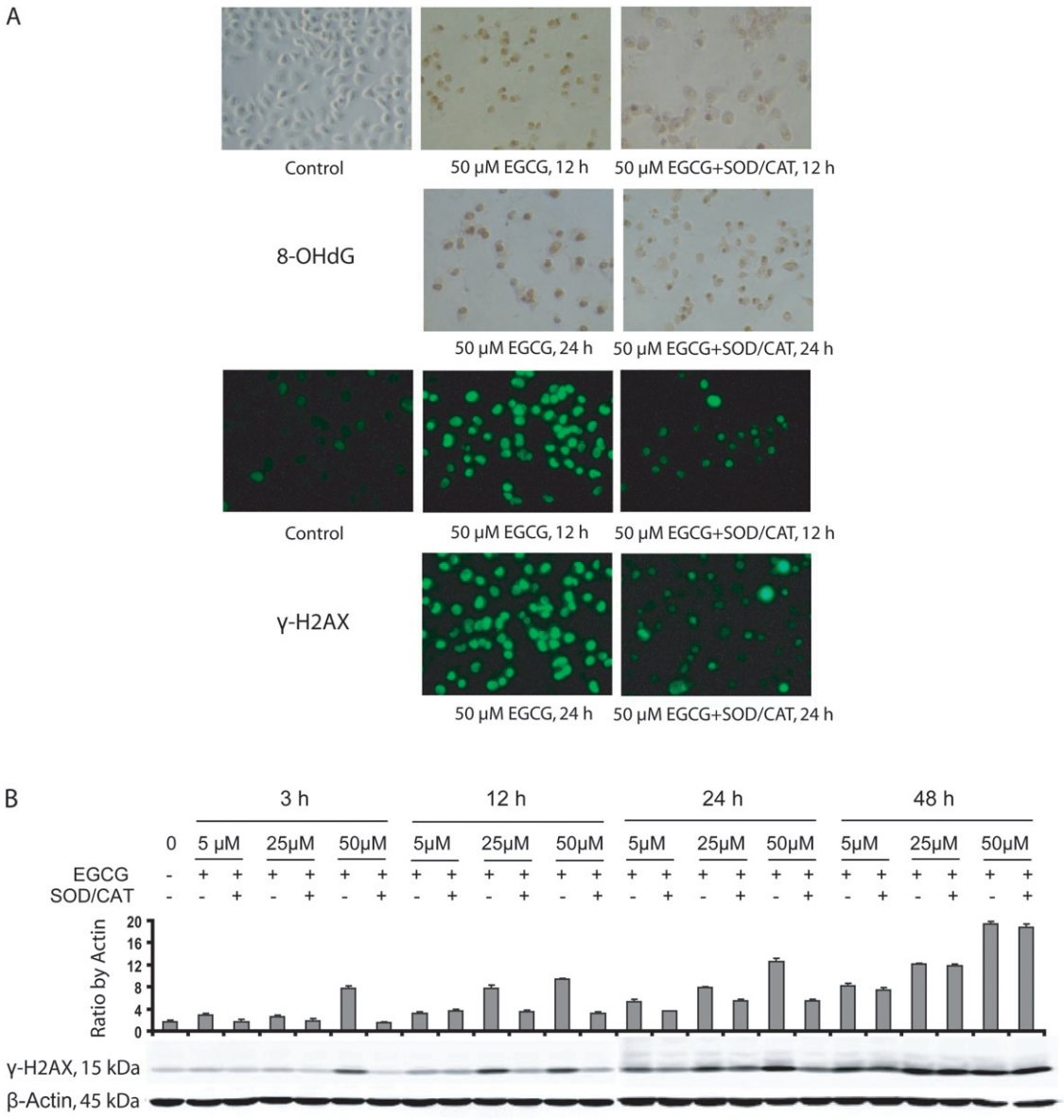

Fig. 6. Effects of EGCG treatments on oxidative stress and DNA damage repair in the H1299 cell lines. The cells were treated with 5–50 μM EGCG for different time periods. (**A**) Representative microphotographs of 8-OHdG- and γ-H2AX-stained cells in the presence of 50 μM EGCG for 12 and 24 h. (**B**) Western blots for γ-H2AX with 5–50 μM EGCG in the presence or absence of SOD/catalase (CAT) (5 U/ml, 30 U/ml) for different time periods. The values shown are mean ± SD.

generation of ROS, which can induce cellular damage and apoptosis (13–16), and this type of action is readily demonstrated in H1299 cells herein. The growth of H1299 cells was dose dependently inhibited, showing an estimated IC_{50} of 20 μM in the MTT assay. The decrease in the number of viable cells was mainly due to apoptosis caused by the EGCG-induced ROS, and most of the EGCG activity was blocked by the presence of SOD/catalase (Figure 4). This is consistent with our previous results on the inhibition of EGCG-induced apoptosis of human lung cancer H661 cells by catalase (15).

A major purpose of this study is to compare the effective concentrations and the mechanisms of action of EGCG in cell culture systems and in animal models. In the animal model, dietary EGCG treatment dose dependently increased the EGCG level in the xenograft tumors and the levels were linearly correlated with the inhibition of tumor growth. Based on the linear regression analysis, an IC_{50} of 0.15 μM was calculated. This concentration *in vivo* is two orders of magnitude lower than the IC_{50} of 20 μM observed *in vitro* (Figure 4). It is commonly observed that the effective concentrations of EGCG observed in cell culture systems are higher than the physiological concentrations measured in animals due to treatment with this agent (31). This raises the question concerning whether the effects of EGCG observed *in vitro* are relevant to the situations *in vivo* (4). In most of the previous studies, however, the *in vitro* and *in vivo* systems are rather different, and the results of the comparison could be misleading. The present parallel *in vitro* and *in vivo* studies produced results that are directly comparable. One possible reason for the observed discrepancy in the effective concentrations between cell culture system and the xenograft model is the short-term exposure to EGCG in the cell culture study (24 h) versus the long-term treatment of animals. It has been reported that prolonging the treatment period can reduce the effective concentration of EGCG in cell culture (32). The generation of more active metabolites of EGCG *in vivo* is also a possibility, even though our previous results indicated that metabolites of tea catechins have lower biological activities than their parent compounds (33,34). The environment for cells in culture is also very different from that in xenograft tumors. In cell culture, the degradation of EGCG generates ROS outside of the cells, which contributes to the induction of apoptosis; whereas in the xenograft model, the ROS in the tumor cells is probably generated mostly inside the cells, and the mechanism for this process remains to be investigated.

The occurrence of intracellular ROS due to the presence of EGCG and decrease by the addition of SOD/catalase were demonstrated in H1299 cells (Figure 5). SOD/catalase markedly reduced ROS generated by 50 μM EGCG at 24 h, but there was still a substantial amount ROS measureable, possibly due to intracellular ROS generated inside the cells. NAC, which serves as an antioxidant both extracellularly and intracellularly, reduced the ROS to the control levels. Similar results were observed on the formation of mitochondrial ROS and mitochondrial membrane potential change. The kinetics of the EGCG-induced formation of ROS, and mitochondrial membrane potential changes, were not significantly different. However, SOD/catalase appeared to be more effective in decreasing intracellular ROS (inhibited by 69.6 ± 0.9%, $n = 3$) than in decreasing mitochondrial ROS (inhibited by 50.7 ± 2.6%, $n = 3$) and membrane potential change (inhibited by 47.9 ± 3.5%, $n = 3$), suggesting that the intracellularly generated ROS play a more important role in causing mitochondrial ROS and membrane potential change.

The generation of oxidative stress in xenograft tumors due to EGCG treatment was demonstrated by the dose-dependent formation of 8-OHdG and γ-H2AX observed, and these events are correlated with the induction of apoptosis (Figure 3). However, the levels of 8-OHdG and γ-H2AX were not elevated by the EGCG treatment in the liver, kidney and lung of the host mice. It is possible that oxidative stress was induced in the tumors by EGCG because H1299 cells possess only low levels of antioxidant enzymes such as hemeoxygenase-1 and the transcription factor NF-E2 related factor-2 (supplementary Figure S1 is available at *Carcinogenesis* Online), which regulates the expression of many antioxidant/detoxification enzymes (35,36). On the other hand, the expression levels of NF-E2 related factor-2 and hemeoxygenase-1 are higher in A549 and HT29 cells (supplementary Figure S1 is available at *Carcinogenesis* Online), and these cells were less responsive to the inhibition by EGCG and the protective action of SOD/catalase (Figure 4). A significant induction of γ-H2AX by EGCG in HT29 cells was not observed by western blot analysis (data not shown). These results are consistent with the report showing that A549 cells confer resistance to apoptosis induction by EGCG *in vitro* because these cells constitutively overexpress hemeoxygenase-1 and its regulating transcription factor, NF-E2 related factor-2 (37).

In summary, the present study demonstrated the inhibitory action of EGCG against cancer cells *in vivo* and *in vitro*, and the effective concentrations of EGCG against H1299 cells in culture are two orders of magnitude higher than those observed in xenograft tumors. The induction of ROS and oxidative DNA damages as well as apoptosis by EGCG was also demonstrated *in vivo* and *in vitro*. EGCG is generally recognized as a strong antioxidant in food chemistry and its antioxidant activity has been demonstrated in some animal and human studies (reviewed in ref. 4). As demonstrated herein, EGCG could also serve as a pro-oxidant in certain circumstances. We suggest that cell apoptosis caused by EGCG-induced ROS and oxidative stress can be an important mechanism for cancer prevention and therapy, especially in systems with low antioxidant capacities.

Supplementary material

Supplementary Figure S1 can be found at http://carcin.oxfordjournals.org/

Funding

National Institutes of Health (CA120915, CA122474, CA128613); National Cancer Institute (CCSG CA72720); NIEHS center (ES05022). National Institutes of Health–American Recover and Reinvestment Act supplement (CA133021-02S1 to A.Y.).

Acknowledgements

We thank Dr Jing Hao for assistance in histologic analysis.

Conflict of Interest Statement: None declared.

References

1. Yang,C.S. *et al*. (1993) Tea and cancer. *J. Natl Cancer Inst.*, **85**, 1038–1049.
2. Lambert,J.D. *et al*. (2005) Inhibition of carcinogenesis by polyphenols: evidence from laboratory investigations. *Am. J. Clin. Nutr.*, **81**, 284S–291S.
3. Yang,C.S. *et al*. (2002) Inhibition of carcinogenesis by tea. *Annu. Rev. Pharmacol. Toxicol.*, **42**, 25–54.
4. Yang,C.S. *et al*. (2009) Cancer prevention by tea: animal studies, molecular mechanisms and human relevance. *Nat. Rev. Cancer*, **9**, 429–439.
5. Naasani,I. *et al*. (2003) Blocking telomerase by dietary polyphenols is a major mechanism for limiting the growth of human cancer cells *in vitro* and *in vivo*. *Cancer Res.*, **63**, 824–830.
6. Nishida,H. *et al*. (1994) Inhibitory effects of (-)-epigallocatechin gallate on spontaneous hepatoma in C3H/HeNCrj mice and human hepatoma-derived PLC/PRF/5 cells. *Jpn. J. Cancer Res.*, **85**, 221–225.
7. Liao,J. *et al*. (2004) Inhibition of lung carcinogenesis and effects on angiogenesis and apoptosis in A/J mice by oral administration of green tea. *Nutr. Cancer*, **48**, 44–53.
8. Wang,D. *et al*. (2004) N-acetyl-seryl-aspartyl-lysyl-proline stimulates angiogenesis *in vitro* and *in vivo*. *Am. J. Physiol. Heart Circ. Physiol.*, **287**, H2099–H105.
9. Xu,Y. *et al*. (1992) Inhibition of tobacco-specific nitrosamine-induced lung tumorigenesis in A/J mice by green tea and its major polyphenol as antioxidants. *Cancer Res.*, **52**, 3875–3879.
10. Liao,S. *et al*. (1995) Growth inhibition and regression of human prostate and breast tumors in athymic mice by tea epigallocatechin gallate. *Cancer Lett.*, **96**, 239–243.
11. Jung,Y.D. *et al*. (2001) EGCG, a major component of green tea, inhibits tumour growth by inhibiting VEGF induction in human colon carcinoma cells. *Br. J. Cancer*, **84**, 844–850.

12. Yang,C.S. *et al*. (2008) Bioavailability issues in studying the health effects of plant polyphenolic compounds. *Mol. Nutr. Food Res.*, **52**(suppl. 1), S139–S51.
13. Hong,J. *et al*. (2002) Stability, cellular uptake, biotransformation, and efflux of tea polyphenol (-)-epigallocatechin-3-gallate in HT-29 human colon adenocarcinoma cells. *Cancer Res.*, **62**, 7241–7246.
14. Hou,Z. *et al*. (2005) Mechanism of action of (-)-epigallocatechin-3-gallate: auto-oxidation-dependent inactivation of epidermal growth factor receptor and direct effects on growth inhibition in human esophageal cancer KYSE 150 cells. *Cancer Res.*, **65**, 8049–8056.
15. Yang,G.Y. *et al*. (1998) Inhibition of growth and induction of apoptosis in human cancer cell lines by tea polyphenols. *Carcinogenesis*, **19**, 611–616.
16. Hou,Z. *et al*. (2004) Effects of tea polyphenols on signal transduction pathways related to cancer chemoprevention. *Mutat. Res.*, **555**, 3–19.
17. Jacobson,M.D. (1996) Reactive oxygen species and programmed cell death. *Trends Biochem. Sci.*, **21**, 83–86.
18. Valavanidis,A. *et al*. (2009) 8-hydroxy-2′ -deoxyguanosine (8-OHdG): a critical biomarker of oxidative stress and carcinogenesis. *J. Environ. Sci. Health C Environ. Carcinog. Ecotoxicol. Rev.*, **27**, 120–139.
19. Barzilai,A. *et al*. (2004) DNA damage responses to oxidative stress. *DNA Repair (Amst.)*, **3**, 1109–1115.
20. Albino,A.P. *et al*. (2004) Induction of H2AX phosphorylation in pulmonary cells by tobacco smoke: a new assay for carcinogens. *Cell Cycle*, **3**, 1062–1068.
21. Burma,S. *et al*. (2001) ATM phosphorylates histone H2AX in response to DNA double-strand breaks. *J. Biol. Chem.*, **276**, 42462.
22. Sarma,K. *et al*. (2005) Histone variants meet their match. *Nat. Rev. Mol. Cell. Biol.*, **6**, 139–49.
23. van Attikum,H. *et al*. (2005) The histone code at DNA breaks: a guide to repair? *Nat. Rev. Mol. Cell Biol.*, **6**, 757–765.
24. Zhou,N. *et al*. (2003) DNA damage-mediated apoptosis induced by selenium compounds. *J. Biol. Chem.*, **278**, 29532–29537.
25. Ovamstrom,O.F. *et al*. (2004) DNA double strand break quantification in-skin biopsies. *Radiother. Oncol.*, **72**, 311–317.
26. Lee,M.J. *et al*. (2000) An improved method for the determination of green and black tea polyphenols in biomatrices by high-performance liquid chromatography with coulometric array detection. *Anal. Biochem.*, **279**, 164–169.
27. Tachibana,H. *et al*. (2004) A receptor for green tea polyphenol EGCG. *Nat. Struct. Mol. Biol.*, **11**, 380–381.
28. Ermakova,S. *et al*. (2005) The intermediate filament protein vimentin is a new target for epigallocatechin gallate. *J. Biol. Chem.*, **280**, 16882–16890.
29. Li,M. *et al*. (2007) Direct inhibition of insulin-like growth factor-I receptor kinase activity by (-)-epigallocatechin-3-gallate regulates cell transformation. *Cancer Epidemiol. Biomarkers Prev.*, **16**, 598–605.
30. He,Z. *et al*. (2008) Fyn is a novel target of (-)-epigallocatechin gallate in the inhibition of JB6 Cl41 cell transformation. *Mol. Carcinog.*, **47**, 172–183.
31. Moiseeva,E.P. *et al*. (2009) Dietary chemopreventive phytochemicals: too little or too much? *Cancer Prev. Res. (Phila Pa)*, **2**, 611–616.
32. Shimizu,M. *et al*. (2005) (-)-Epigallocatechin gallate and polyphenon E inhibit growth and activation of the epidermal growth factor receptor and human epidermal growth factor receptor-2 signaling pathways in human colon cancer cells. *Clin. Cancer Res.*, **11**, 2735–2746.
33. Lu,H. *et al*. (2003) Enzymology of methylation of tea catechins and inhibition of catechol-O-methyltransferase by (-)-epigallocatechin gallate. *Drug Metab. Dispos.*, **31**, 572–579.
34. Lambert,J.D. *et al*. (2005) Synthesis and biological activity of the tea catechin metabolites, M4 and M6 and their methoxy-derivatives. *Bio org. Med. Chem. Lett.*, **15**, 873–876.
35. Itoh,K. *et al*. (1997) An Nrf2/small Maf heterodimer mediates the induction of phase II detoxifying enzyme genes through antioxidant response elements. *Biochem. Biophys. Res. Commun.*, **236**, 313–322.
36. Nguyen,T. *et al*. (2004) The pathways and molecular mechanisms regulating Nrf2 activation in response to chemical stress. *Free Radic. Biol. Med.*, **37**, 433–441.
37. Kweon,M.H. *et al*. (2006) Constitutive overexpression of Nrf2-dependent heme oxygenase-1 in A549 cells contributes to resistance to apoptosis induced by epigallocatechin 3-gallate. *J. Biol. Chem.*, **281**, 33761–33772.

Received November 25, 2009; revised January 8, 2010; accepted February 9, 2010